

Characterization of Magnesium Porphyrins and Aggregation of Porphyrins in Organic Solvent

Xiaoyong Zhang, Ken Sasaki, and Yasuhisa Kuroda*

Department of Biomolecular Engineering, Kyoto Institute of Technology, Matsugasaki, Sakyo-ku, Kyoto 606-8585

Received May 8, 2006; E-mail: ykuroda@kit.ac.jp

Magnesium tetrakis(4-sulfonatophenyl)porphyrin complex was synthesized and purified. MgTPPS (tetrasodium salt) and MgTPPSC8 (tetraoctylammonium salt) showed unique spectroscopic behaviors in an aqueous buffer and CH₃OH respectively, indicating solvent ligation on the Mg ion. In pure CH₂Cl₂, the MgTPPSC8 formed unique J-type oligomers, in which the sulfonato groups mutually coordinate to the vicinal Mg ion. In binary solvent systems of CH₂Cl₂ and CH₃OH, MgTPPSC8 formed H-aggregates as well as other TPPS derivatives, and aggregation was controlled by changing the ratio of the solvents. The geometrical structure of J-type oligomers was estimated by using the exciton point-dipole coupling theory.

Porphyrin is one of the most ubiquitous compounds found in nature, and it plays important roles in a wide variety of biochemical processes, such as oxygen retention and delivery, various enzymatic redox reactions, or the conversion of light energy to chemical energy. Thus, porphyrins and related molecules have attracted strong interest as the subject of extensive chemical investigations because of their potential usefulness in technological applications such as biomimetic catalysts,¹ sensors,² optoelectronic devices,³ photodynamic therapy,⁴ molecular logic devices,⁵ and artificial solar energy harvesting and storage systems.⁶

In order to clarify the detailed mechanisms of the reactions mediated by natural porphyrin molecules, various types of synthetic porphyrins and their metal complexes have been prepared. Tetraphenylporphyrin (TPP) is the most widely used artificial porphyrin and a variety of modified TPPs have been synthesized according to the target functions. Tetrakis(4-sulfonatophenyl)porphyrin (TPPS) is a member of the TPP family and has been sometimes utilized as a water soluble porphyrin. Metal complexes of TPPS, such as ZnTPPS and FeTPPS, have been also widely studied as biomimetic model compounds.⁷ Systematic studies on the magnesium complex of TPPS, however, are surprisingly rare,⁸ in spite of the essential importance of the Mg complexes, such as chlorophyll and bacteriochlorophyll, in photosynthetic systems. The one of the reasons for the scarcity of the studies on MgTPPS may be that it easily undergoes demetallation in aqueous medium,⁹ and therefore, it is somewhat difficult to purify. For example, an erroneous electronic spectrum has been reported,¹⁰ and the spectroscopic details of commercially available MgTPPS are not clear.

In this work, we report the preparation of pure MgTPPS, its spectroscopic properties and unique medium dependent aggregation behavior, which was found by changing the counter ions of the sulfonate groups of TPPS with highly hydrophobic tetraoctylammonium ion. These properties are discussed in comparison with those of related porphyrins shown in Chart 1.

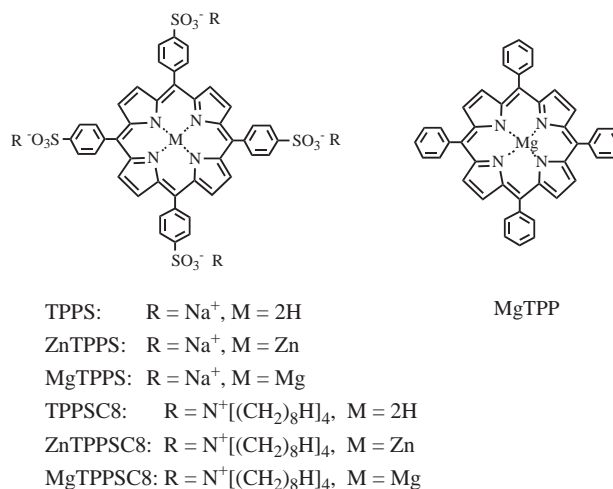


Chart 1. Molecular structures and abbreviations of this work.

Experimental

Materials. Free-base TPPS and TPP were obtained from Nacalai Tesque. Spectroscopic grade methanol and dichloromethane (Nacalai Tesque) were used for all spectroscopic measurements.

Apparatus. Absorption and fluorescence spectra were recorded on a Shimadzu MultiSpec-1500 and a Hitachi F-4500 fluorescence spectrophotometer, respectively. Resonance light scattering (RLS) spectra were obtained by scanning simultaneously with excitation and emission monochromators of an F-4500 spectrophotometer with a slit width of 2.5 nm both for the excitation and emission. All of the RLS spectra were corrected by subtracting the corresponding black sample, but not corrected for the absorption of the samples. The sample holder of the instruments was kept at 298 K. Dynamic light scattering (DLS) measurements were obtained on a DLS-7000 (Otsuka) fitted with a 75 mW Ar laser (488 nm). The DLS data were collected with scattering angles of $\theta = 60, 90,$ and 120° , analyzed by a discrete multiexponential

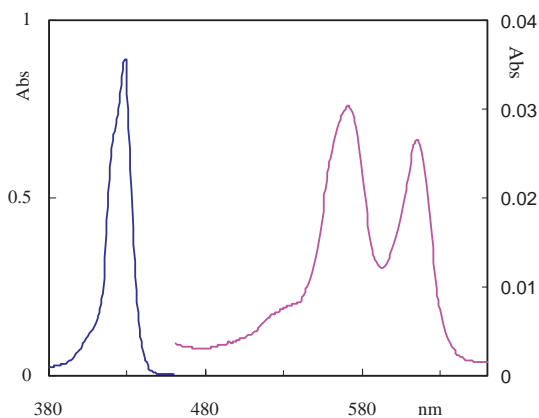


Fig. 1. The absorption spectrum of MgTPPS (2×10^{-6} M) in buffer at 298 K.

least-squares fit (NNLS) and, in almost all cases, were fitted by setting the major contribution to be at about 100 nm (D_H) and the minor contribution centered at several nanometers. ^1H NMR spectra (500 MHz) were obtained on a BRUKER ARX-500 spectrometer.

Preparation of MgTPP, MgTPPS, and ZnTPPS. Metallation reactions were carried out according to the procedures of Adler et al.¹¹ Identification of MgTPP and ZnTPPS was confirmed by measuring their ^1H NMR and UV–visible spectra, which were consistent with those described in the literature.¹² MgTPPS was prepared by refluxing free-base TPPS (0.27 g) with magnesium chloride (0.18 g) and NaOH (0.13 g) overnight in DMF (50 mL). MgTPPS was purified by recrystallization with two times methanol–tetrahydrofuran. Anal. Found: C, 45.75; H, 3.57; N, 4.66; Mg, 1.99% (This Mg content was determined by atomic absorption spectrometry). Calcd for $\text{C}_{44}\text{H}_{37}\text{N}_4\text{O}_{18.5}\text{S}_4\text{Na}_4\text{Mg}$ (MgTPPS $\cdot 6.5\text{H}_2\text{O}$): C, 45.47; H, 3.21; N, 4.82; Mg, 2.09%. ESI-MS (m/z): 1022.3 ($[\text{MgTPPS} - \text{Na}^+]^-$, calcd 1022.2). UV–vis: λ_{max} (nm, buffer, 298 K) ($\epsilon/\text{L mol}^{-1} \text{cm}^{-1}$) 446000 (428 nm), 14700 (571 nm), 12700 (615 nm). To avoid demetallization of MgTPPS in a non-alkaline aqueous solution, the experiments were carried out in sodium carbonate–sodium bicarbonate buffer solution at pH 10.

MgTPPSC8 was obtained by extracting the MgTPPS aqueous solution with a CHCl_3 solution of the tetra-*n*-octylammonium bromide. Although the ^1H NMR analysis shows that the product contains 5.2 molecules of the tetra-*n*-octylammonium moiety in one MgTPPS, the product was used for the present measurement without further purification, because an appropriate method to remove the excess counter ion could not be found. UV–vis: λ_{max} (nm, CH_2Cl_2 , 298 K) ($\epsilon/\text{L mol}^{-1} \text{cm}^{-1}$) 528000 (427 nm), 27000 (566 nm), 15800 (607 nm). ZnTPPSC8 and TPPSC8 were prepared like MgTPPSC8.

Results

MgTPPS in Water. As expected, MgTPPS is easily demetallated in neutral and acidic aqueous solutions.^{9,10} For example, its half-life was ca. 20 min even in neutral distilled water. Therefore, all of the experimental data for MgTPPS in an aqueous solution were collected in basic solutions (pH 10). Figure 1 shows the absorption spectrum of MgTPPS in a buffer solution. The spectrum of MgTPPS had a Soret band at 428 nm and a shoulder at 423 nm. Interestingly, the Soret band of MgTPPS was dependent on the solution temperature (283–

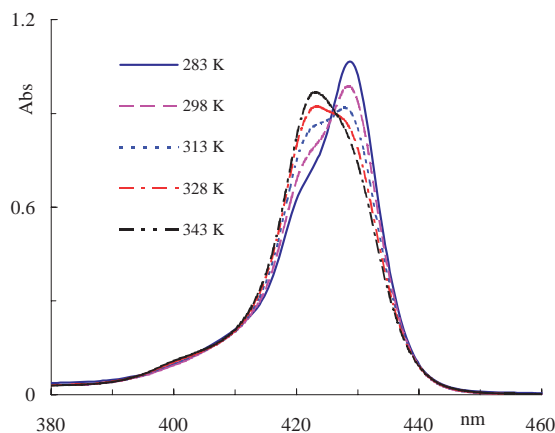


Fig. 2. The absorption spectra of MgTPPS (2.2×10^{-6} M) versus temperature in buffer.

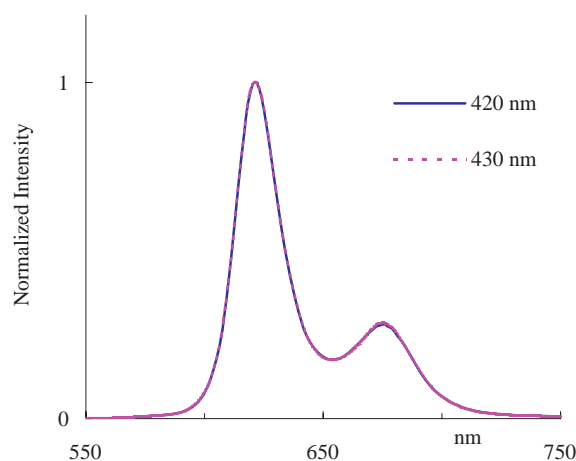


Fig. 3. Fluorescence emission spectra of MgTPPS (1×10^{-6} M) in buffer at 298 K, excited at 420 and 430 nm.

343 K) as shown in Fig. 2, although that of the isoelectronic metal porphyrin ZnTPPS (421 nm) was not. The presence of the isosbestic point at 426 nm in the variable temperature spectra of the MgTPPS indicated the existence of two species in thermal equilibrium. Since no spectral modifications due to a change in the pH (9–11) were found, the observed equilibrium is not thought to originate from the simple proton-transfer process. Furthermore, the absorption spectrum was not dependent on the concentration in the range of 4×10^{-7} – 2×10^{-5} M at 298 K. The results suggest that the observed spectral behavior is not due to the change in the aggregation state, such as oligomer formation.

In contrast to the present dual spectral behavior, the emission spectra observed after excitation at 420 and 430 nm were basically the same fluorescence as shown in Fig. 3. Furthermore, the fluorescence emission decay of the MgTPPS in buffer measured after excitation at 560 nm had a single exponential profile with a lifetime of 7.1 ns, which is consistent with the fact that only a single fluorescence spectrum was observed, despite MgTPPS having two ground states.

One of the most plausible explanations for the present observation is the coordination of a water molecule to the Mg atom.¹³ Since MgTPP has been shown to have one molecule

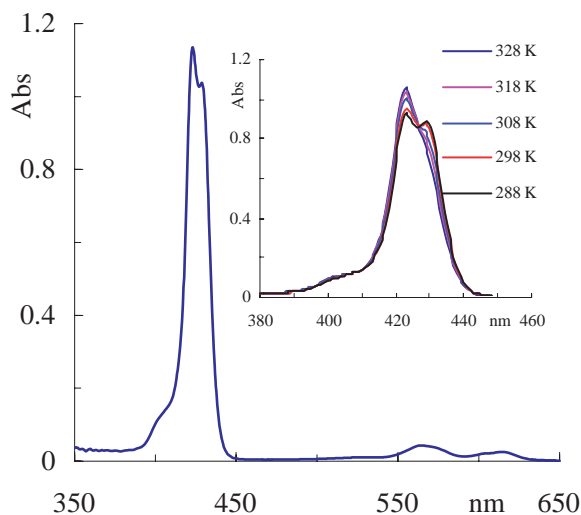


Fig. 4. Absorption spectrum of MgTPPSC8 (2×10^{-6} M) in CH_3OH at 298 K; inset: the spectra by changing its temperature in CH_3OH .

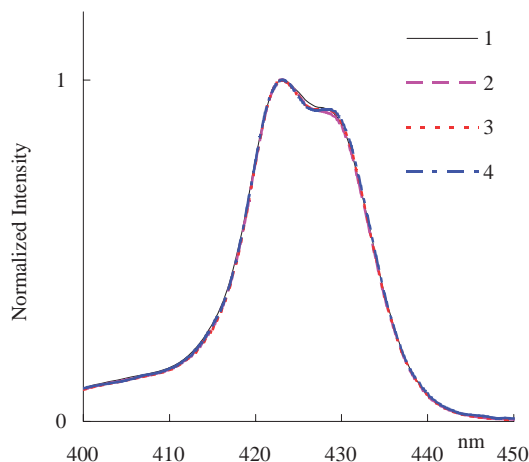


Fig. 5. Absorption spectra of MgTPPSC8 in CH_3OH at 298 K, 1: 1.6×10^{-5} M, 2: 1.2×10^{-5} M, 3: 1.6×10^{-6} M, 4: 1.6×10^{-7} M.

of water in the state from the X-ray diffraction study by Timkovich and Tulinsky,¹⁴ it is possible that, in buffer, MgTPPS exists in equilibrium with water. This type of the coordination change will be discussed in relation to that of CH_3OH later.

MgTPPSC8 in Organic Solvent. Absorption Spectrum and Fluorescence Emission Spectrum in CH_3OH : MgTPPSC8 having hydrophobic counter ions was soluble in various organic solvents. The absorption spectrum of MgTPPSC8 in CH_3OH is shown in Fig. 4. The Soret band in CH_3OH was at $\lambda_{\text{max}} = 423$ nm and had a shoulder at 429 nm, and the Q-band was also not a single component. Upon changing the temperature of the solution, a remarkable change of the absorption spectra is induced. In addition, as shown in Fig. 5, its shape was not dependent on the porphyrin concentration in the range of 1.6×10^{-7} – 1.6×10^{-5} M. The fluorescence emission spectra were not affected by the excitation wavelength, and the fluorescence decay had a single exponential profile with a lifetime of 7.8 ns. Since all of these observa-

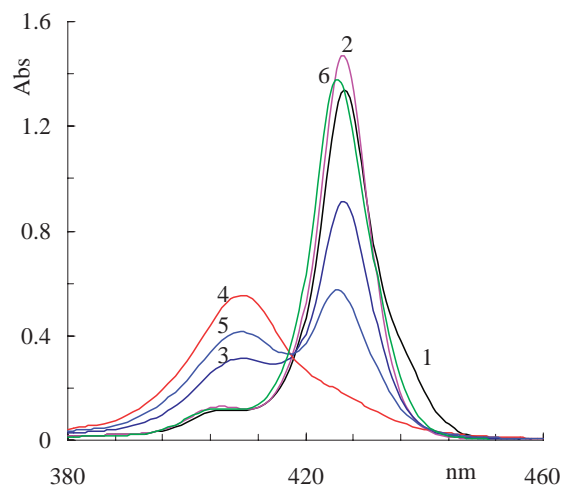


Fig. 6. Absorption spectra of MgTPPSC8 (2.1×10^{-6} M) in CH_2Cl_2 upon addition of CH_3OH at 298 K. $\omega = \text{CH}_3\text{OH}/\text{CH}_2\text{Cl}_2$ (v/v), 1: $\omega = 0$, 2: $\omega = 0.0017$, 3: $\omega = 0.03$, 4: $\omega = 0.1$, 5: $\omega = 0.2$, 6: $\omega = 0.4$.

tions indicate the ligation of CH_3OH , in order to confirm this possibility, the spectroscopic titration of MgTPP with CH_3OH in CH_2Cl_2 was carried out. The results indicate that the coordination of CH_3OH consists of two-step equilibrium with equilibrium constants at 295 ± 75 and $15 \pm 3 \text{ M}^{-1}$. Thus, the MgTPPSC8 in CH_3OH is considered to be in equilibrium with a solvent coordinated species, such as $\text{MgTPP}(\text{CH}_3\text{OH})_2$, of which the crystal structure has been reported by McKee and Rodley.¹⁵

In pure CH_2Cl_2 , the spectrum of MgTPPSC8 had a Soret band at λ_{max} 427 nm with a shoulder at 437 nm, and Q-bands were observed at $\lambda_{\text{max}} = 566$ and 607 nm (Fig. 6). The absorption spectra of MgTPPSC8, however, exhibited complex behavior with respect to changes in the experimental conditions (Fig. 6). Addition of a small amount of CH_3OH (5 μL) to 3 mL CH_2Cl_2 ($\omega(\text{CH}_3\text{OH}/\text{CH}_2\text{Cl}_2 \text{ v/v}) = 0.0017$) containing 2.1×10^{-6} M MgTPPSC8 resulted in the disappearance of the shoulder at 437 nm and an increase in the peak intensity at $\lambda_{\text{max}} = 427$ nm without notable change in the Q-band region. The shoulder also disappears in CH_2Cl_2 saturated with H_2O . The relative strength of this shoulder in pure CH_2Cl_2 increased upon an increase in the concentration of MgTPPSC8, which indicates the formation of self-aggregates of MgTPPSC8. In addition, MgTPP did not show a red-shifted shoulder. Thus, these results suggest the association and dissociation of the MgTPPSC8 molecules accompanying a change in ligation is a plausible mechanism for the observed spectroscopic behavior. In pure CH_2Cl_2 , one of the sulfonatos on the porphyrin may coordinate to the central Mg ion of another porphyrin to form a slipped and stacked association (J-type oligomer¹⁶) that can be a dimer or a small oligomer as shown in Fig. 7, for which the observed red-shift values were in good agreement with that estimated by the exciton point-dipole coupling theory as shown in later section. On addition of CH_3OH , the sulfonato ligand was replaced by CH_3OH molecule, and the oligomer dissociated into monomers, which give clear Soret and Q band absorption.

Interestingly, after the J-type oligomer was destroyed to

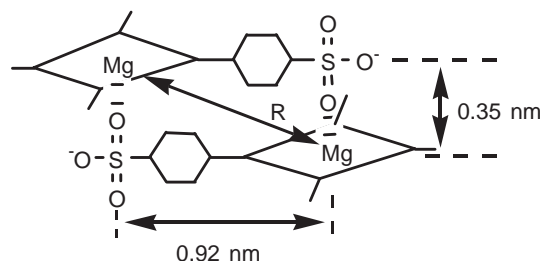


Fig. 7. J-Type dimer model of MgTPPSC8 in CH_2Cl_2 .

give monomers by addition of a small amount of CH_3OH , further addition of CH_3OH resulted in further changes in the absorption spectra of MgTPPSC8 as shown in Fig. 6. In other words, the monomeric peak in the Soret band decreased, and a new broad band with the maximum located around 409 nm appeared. When the methanol ratio (ω) was 0.1, the peak due to monomer disappeared, and the solutions became slightly turbid. This is a feature of the formation of very large H-aggregates, which is characterized by a blue-shifted Soret band.¹⁶

When $\omega > 0.1$, the intensity of the new band corresponding to H-aggregates state decreased continuously, and the band for the monomer region was recovered (Fig. 6). No further change is observed both in the region of the H-aggregate and the region of monomer over $\omega \approx 0.4$. Finally, when ω was extremely large, the spectrum becomes similar to that in pure CH_3OH .

These processes were shown to be reversible. After evaporation of the solvent from the H-aggregate solution, the residual porphyrin showed the same spectroscopic changes as described above. The results indicate that the complicated observations were not due to irreversible formation of some structurally different porphyrin derivatives of MgTPPS.

Resonance Light Scattering Spectra. Resonance light scattering (RLS) developed by Pasternack and Collings is a powerful tool to detect the presence of electronically coupled porphyrin aggregates and to study its size.¹⁷ For example, in the porphyrin RLS spectrum, the formation and the structure of the J-aggregates of TPPS in an acidic aqueous solution has been observed.¹⁸ In the RLS measurement, simultaneous scanning of excitation and emission wavelengths results in a strongly enhanced light scattering profile for the large aggregates, while no such scattering is observed for porphyrin monomers and small oligomers.¹⁷

As shown in Fig. 8, the solution of MgTPPSC8 in pure CH_2Cl_2 , exhibited no extensive scattering in the monomer region (≈ 427 nm) and in the J-type oligomer one (≈ 437 nm), indicating that the size of the J-type oligomer is very small. When ω was at 0.0017, at which the J-type oligomer breaks into monomers, no enhanced light scattering was obtained. In contrast, upon further addition of CH_3OH up to $\omega = 0.4$, an intense RLS signal was observed at the position of the blue-shifted band corresponding to the H-aggregates but not at that of the monomer band, even though the maximum absorption intensity of the H-aggregates was just 1/3 of that of the monomers. Then, the intensity of RLS spectrum became weak again when $\omega > 0.4$, suggesting that the MgTPPSC8 molecule exists as the monomer or small aggregate.

We also measured the RLS spectra of MgTPPS in an aque-

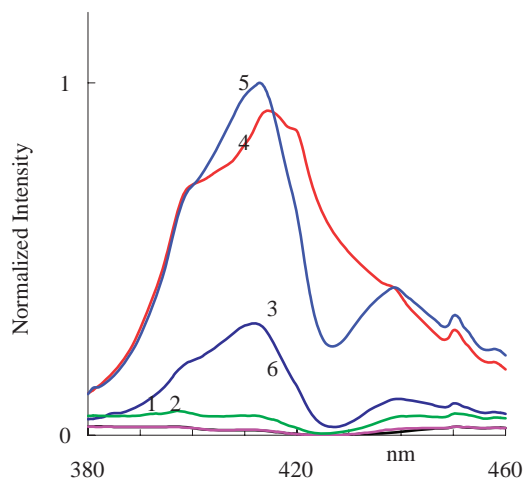


Fig. 8. RLS spectra of MgTPPSC8 (2.1×10^{-6} M) in CH_2Cl_2 upon addition of CH_3OH at 298 K. 1: $\omega = 0$, 2: $\omega = 0.0017$, 3: $\omega = 0.03$, 4: $\omega = 0.1$, 5: $\omega = 0.2$, 6: $\omega = 0.4$.

ous buffer and of MgTPPSC8 in CH_3OH . However, no enhanced light scattering was observed for either, indicating that the species under these conditions does not involve large size aggregates.

In order to determine the origin of the aggregate formation in the CH_2Cl_2 - CH_3OH system, we investigated the aggregation behavior of the MgTPP, TPPSC8, and ZnTPPSC8.

The non-ionic porphyrin magnesium complex, MgTPP, showed a sharp Soret band in CH_2Cl_2 , without a shoulder, like MgTPPSC8 in CH_2Cl_2 , and in CH_3OH , a double Soret band with $\lambda_{\text{max}} = 421$ nm and a shoulder at around 428 nm was observed. Furthermore, the temperature dependence of the absorption spectrum of MgTPP in CH_3OH is similar to that of MgTPPSC8. The observations again support that CH_3OH coordinates to MgTPP as suggested by McKee and Rodley.¹⁵ However, in contrast with MgTPPSC8, MgTPP in CH_2Cl_2 did not show enhanced light scattering effect upon addition of any amount of CH_3OH , and no change in its electronic spectra, except for just a slight red shift was observed. Thus, it was concluded that MgTPP aggregates do not form in these solvents and that the Mg ions do not participate in the formation of H-aggregates formation of MgTPPSC8.

Another interesting feature of the MgTPPSC8 aggregation was obtained from a spectroscopic comparison with ZnTPPSC8 and TPPSC8. As shown in Fig. 9, the absorption spectrum of TPPSC8 in CH_2Cl_2 exhibited a Soret band at $\lambda_{\text{max}} = 419$ nm without an apparent shoulder peak, and upon addition of CH_3OH , a new broad and blue-shifted band around 406 nm appeared. The monomeric Soret band basically disappeared at $\omega = 0.1$. Upon further addition of CH_3OH up to $\omega = 0.5$, the blue-shifted band disappeared, and the monomeric Soret band reappeared, which is similar to the behavior of MgTPPSC8 described above. The RLS spectroscopic characteristics of TPPSC8 and ZnTPPSC8 also very similar to those of MgTPPSC8 (Fig. 10), suggesting that H-aggregates form with the TPP derivatives having sulfonate groups regardless the central metal.

On the other hand, it should be noted that neither TPPSC8

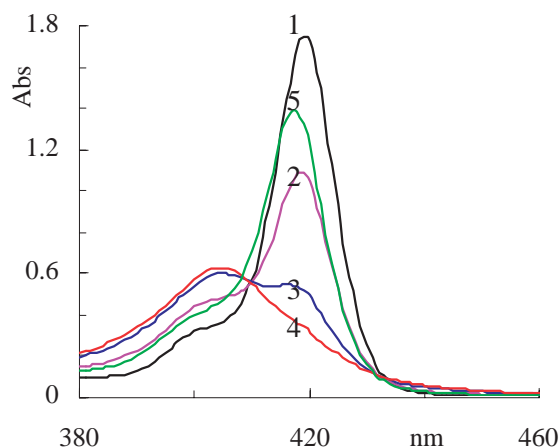


Fig. 9. The absorption spectra of TPPSC8 (3.8×10^{-6} M) in CH_2Cl_2 upon addition of CH_3OH at 298 K. 1: $\omega = 0$, 2: $\omega = 0.05$, 3: $\omega = 0.08$, 4: $\omega = 0.1$, 5: $\omega = 0.5$.

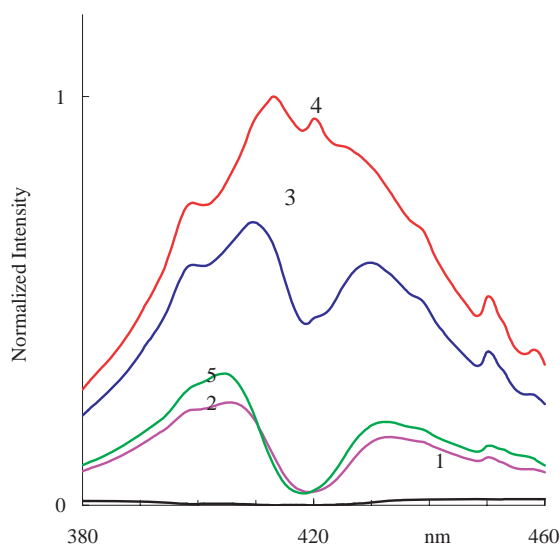


Fig. 10. RLS spectra of TPPSC8 (3.8×10^{-6} M) in CH_2Cl_2 upon addition of CH_3OH at 298 K. 1: $\omega = 0$, 2: $\omega = 0.05$, 3: $\omega = 0.08$, 4: $\omega = 0.1$, 5: $\omega = 0.5$.

and ZnTPPSC8 nor MgTPP formed J-aggregates as shown in the absorption at ≈ 437 nm. These results indicate that both Mg metal and sulfonato groups are essential for the formation of J-aggregates.

^1H NMR Spectra. Aggregation of porphyrins and chlorophylls in solutions has been widely studied by NMR spectrum.¹⁹ Because NMR is a relatively insensitive technique, it is generally necessary to record spectra at much higher concentrations than those ordinarily used for UV-vis absorption spectroscopy. Therefore, the equilibrium involving the TPPS derivatives observed by NMR is expected to favor the formation of aggregates. As shown in Fig. 11, the signal of the phenyl protons was broad in pure CDCl_3 . Titration of a MgTPPSC8 (4 mM) solution with the CD_3OD resulted in a remarkable sharpening of the phenyl proton signals up to $\omega \approx 0.03$, where the signals show the clear AX-like pattern similar to that observed in pure CD_3OD . The observations correspond to the dissociation of J-aggregates into the monomers of MgTPPSC8

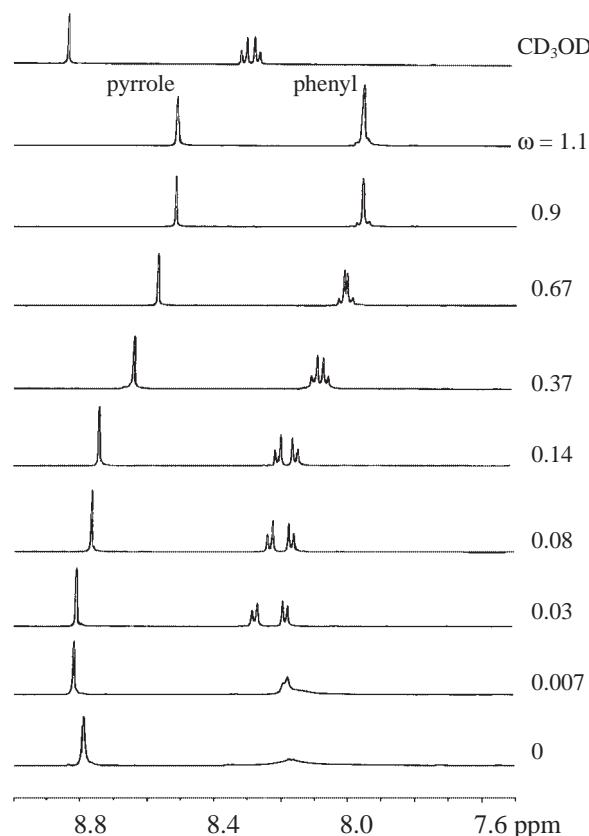


Fig. 11. ^1H NMR spectra of MgTPPSC8 (4×10^{-3} M) in CDCl_3 , CD_3OD , and $\text{CD}_3\text{OD}/\text{CDCl}_3$ ($\omega = v/v$) at 298 K.

discussed above. Upon further addition of CD_3OD , signals of pyrrole and phenyl protons shifted further upfield accompanied by a change in the coupling pattern. Two sets of signals due to the phenyl groups converged into a singlet-like signal at $\omega = 0.9$, which is quite different from that of AX-like pattern observed in pure CD_3OD . It is reasonable to assign this characteristic change in NMR signals to the second process from the monomeric state to H-aggregates of MgTPPSC8. It should be noted that the proton signals of H-aggregates are much sharper than that of J-aggregates, which may suggest that the MgTPPSC8 molecules in the J-aggregates are more strongly restricted than those in the H-aggregates. However, a direct comparison between the aggregate formation under an electro-spectroscopic conditions and that under NMR conditions is still unclear because of the large difference in the porphyrin concentrations.

Dynamic Light Scattering. The DLS technique is commonly used to determine the hydrodynamic diameter of submicrometric dispersed particles by measuring their diffusion coefficients.²⁰ In this work, solutions of MgTPPSC8, ZnTPPSC8, and TPPSC8 in $\text{CH}_3\text{OH}/\text{CH}_2\text{Cl}_2$ at $\omega = 0.1$, at which H-aggregates are expected, were investigated with this technique.

The analyses of obtained scattering data showed that major part of all TPPS derivatives form relatively large and uniform aggregates and the average hydrodynamic diameters (D_H) of the H-aggregates of TPPSC8, ZnTPPSC8, and MgTPPSC8 were determined to be 106, 154, and 110 nm, respectively, in $\text{CH}_3\text{OH}/\text{CH}_2\text{Cl}_2$.

Solvent	CH ₂ Cl ₂	Mixture of CH ₂ Cl ₂ and CH ₃ OH	CH ₃ OH
MgTPPSC8	J-type oligomer	monomer with CH ₃ OH ligand ^{a)}	monomer with CH ₃ OH ligand ^{b)}
ZnTPPSC8 and TPPSC8	monomer without J-aggregate	monomer ^{c)}	monomer ^{c)}
MgTPP	monomer in all solvent systems ^{d)}		

a) The most plausible species is 5-coordinate one. b) The most plausible species is 6-coordinate one. c) The ligation states are not clear. d) CH₃OH ligation states change according to a two step equilibrium, see text.

Scheme 1. Transformation of porphyrin derivatives in various solvents.

Discussion

The TPPS derivatives that became soluble in organic solvents by addition of highly hydrophobic counter ions, i.e., tetraoctylammonium cation, show the interesting transformation of the aggregation states according to the solvent compositions as described above. The observations are summarized in Scheme 1. The structure of chromophore aggregates ranging from dimer to oligomers has been described in the literature by using the UV-vis spectroscopic data of the relating monomers.²¹ The exciton point-dipole coupling theory developed by Kasha et al. has been used to provide a qualitative explanation of the electronic spectra differences between monomer and aggregates.²²

Since this relationships has been successfully applied not only to the simple hydrocarbon systems but also to larger scale systems such as porphyrin assemblies,²³ the relative geometric arrangement of porphyrins in the present aggregation systems was estimated by using this model based on the unit geometry reported by Hunter and Sanders²⁴ shown in Fig. 7.

Using the observed coupling energy and these geometric assumptions, the *R* value for the J-type oligomer of MgTPPSC8 was evaluated to be ca. 9.8 Å. This geometrical value agrees with that of the dimer model where sulfonato groups mutually coordinate to Mg ion as shown in Fig. 7. Interestingly, the dimension of this porphyrin dimer is similar to those proposed for the chlorophyll *a* dimer by Katz et al.²⁵ and vicinal chlorophylls in LH systems.²⁶

The TPPS derivatives TPPSC8, MgTPPSC8, and ZnTPPSC8 may self-associate to form the H-aggregates at $\omega = 0.1$. In contrast, MgTPP did not form this type of aggregate. It indicates that sulfonato groups and tetra-*n*-octylammonium counter ions are needed requirements for H-aggregates formation. Although the geometrical structure of these H-aggregates are expected to be practically same for all cases because of their similar coupling energies and hydrodynamic diameters, reliable structure estimation assuming the exciton coupling mechanism may be difficult because the size of the aggregates is too large. It, however, should be noted that the apparent hydrodynamic diameters (≈ 100 nm), observed for the H-aggregates seem to be too big to allow significant electronic interactions among porphyrins, if the porphyrin mole-

cules are distributed uniformly throughout these particles. A plausible model for the present H-aggregates is a reverse micelle-like model where the lipophilic TPPSC8 molecules are adsorbed on the surface of a methanol rich micro droplet. For further elucidation for the structures of the H-aggregates, more detailed investigations are needed.

Conclusion

We synthesized and purified MgTPPS. The MgTPPS derivatives showed unique spectroscopic behavior in an aqueous buffer and CH₃OH, indicating that the solvent coordination to Mg ion. In pure CH₂Cl₂, MgTPPSC8 formed J-type oligomers, in which the sulfonato groups seem to coordinate mutually to the vicinal magnesium ions. In CH₂Cl₂ and CH₃OH, these lipophilic porphyrins may encapsulate the polar methanol micelles as a surfactant and form particles in which porphyrins are regularly assembled on the surface.

Supporting Information

Spectral change of Q-band of MgTPPS in buffer versus temperature, spectral change of MgTPPS in buffer upon addition of NaOH solution, titration spectra of MgTPP in CH₂Cl₂ versus CH₃OH, absorption spectral change and RLS spectral change of ZnTPPSC8 in CH₂Cl₂ upon addition of CH₃OH. This material is available free of charge on the web at <http://www.csj.jp/journals/bcsj/>.

References

- 1 M. Mansuy, *Pure Appl. Chem.* **1990**, 62, 741.
- 2 W. Qin, P. Parzuchowski, W. Zhang, M. E. Meyerhoff, *Anal. Chem.* **2003**, 75, 332.
- 3 a) R. K. Lammi, A. Ambroise, T. Balasubramanian, R. W. Wagner, D. F. Bocian, D. Holten, J. S. Lindsey, *J. Am. Chem. Soc.* **2000**, 122, 7579. b) P. A. Liddell, G. Kodis, A. L. Moore, T. A. Moore, D. Gust, *J. Am. Chem. Soc.* **2002**, 124, 7668.
- 4 W. R. Dichtel, J. M. Serin, C. Edder, J. M. J. Frechet, M. Matuszewski, L.-S. Tan, T. Y. Ohulchanskyy, P. N. Prasad, *J. Am. Chem. Soc.* **2004**, 126, 5380.
- 5 S. D. Straight, J. Andréasson, G. Kodis, S. Bandyopadhyay, R. H. Mitchell, T. A. Moore, A. L. Moore, D. Gust, *J. Am. Chem. Soc.* **2005**, 127, 9403.
- 6 Y. Kuroda, K. Sugou, K. Sasaki, *J. Am. Chem. Soc.* **2000**,

122, 7833.

7 a) Y. Saiki, Y. Amao, *Biotechnol. Bioeng.* **2003**, 82, 710. b) B. O. Fernandez, I. M. Lorkovic, P. C. Ford, *Inorg. Chem.* **2003**, 42, 2. c) V. E. Yushmanov, *Inorg. Chem.* **1999**, 38, 1713.

8 a) A. Harriman, P. Neta, M.-C. Richoux, *J. Phys. Chem.* **1986**, 90, 3444. b) H. van Willigen, M. H. Ebersole, *J. Am. Chem. Soc.* **1987**, 109, 2299. c) G. S. Nahor, P. Neta, P. Hambright, A. N. Thompson, A. Harriman, *J. Phys. Chem.* **1989**, 93, 6181. d) M. Kumar, P. Neta, T. P. G. Sutter, P. Hambright, *J. Phys. Chem.* **1992**, 96, 9571. e) P. Kubát, J. Mosinger, *J. Photochem. Photobiol., A* **1996**, 96, 93.

9 H. R. Jiménez, M. Julve, J. Faus, *J. Chem. Soc., Dalton Trans.* **1991**, 1945.

10 A. Berg, M. Rachamim, T. Galili, H. Levanon, *J. Phys. Chem.* **1996**, 100, 8791. They have reported that MgTPPS exhibited four distinctive peaks at 516, 564, 602, and 642 nm with relative intensities of 4.5:5.6:3.2:1, respectively in dimethylsulfoxide–glycerol (1:1). However, using that conditions that they used, we obtained a remarkably different result, i.e., peaks at 525, 565, and 605 nm, with relative intensities of 1:6.2:3.3, respectively. Since we could get a really similar absorption spectrum in comparison with their data by adding free base TPPS into the MgTPPS solution, we assumed that the demetallation of the MgTPPS occurred in their sample.

11 A. D. Adler, F. R. Longo, V. Varadi, *Inorg. Synth.* **1976**, 16, 213.

12 a) J. S. Lindsey, J. N. Woodford, *Inorg. Chem.* **1995**, 34, 1063. b) K. Kalyanasundaram, M. Neumann-Spallart, *J. Phys. Chem.* **1982**, 86, 5163.

13 Since the electronic spectra of MgTPPS in H₂O show spectral change only above pH 13, the ligand for this ligation is expected to be H₂O in the present experimental conditions of pH 8–12.

14 R. Timkovich, A. Tulinsky, *J. Am. Chem. Soc.* **1969**, 91,

4430.

15 V. McKee, G. A. Rodley, *Inorg. Chim. Acta* **1988**, 151, 233.

16 N. Micali, F. Mallamace, A. Romeo, R. Purrello, L. Monsù Scolaro, *J. Phys. Chem. B* **2000**, 104, 5897.

17 R. F. Pasternack, P. J. Collings, *Science* **1995**, 269, 935.

18 P. J. Collings, E. J. Gibbs, T. E. Starr, O. Vafek, C. Yee, L. A. Pomerance, R. F. Pasternack, *J. Phys. Chem. B* **1999**, 103, 8474.

19 a) R. J. Abraham, F. Eivazi, H. Pearson, K. M. Smith, *J. Chem. Soc., Chem. Commun.* **1976**, 698. b) R. J. Abraham, F. Eivazi, H. Pearson, K. M. Smith, *J. Chem. Soc., Chem. Commun.* **1976**, 699. c) N. C. Maiti, S. Mazumdar, N. Periasamy, *J. Phys. Chem.* **1998**, 102, 1528.

20 B. J. Berne, R. Pecora, *Dynamic Light Scattering*, Wiley, New York, **1976**.

21 a) H. Garcia-Ortega, J. L. Bourdelande, J. Crusats, Z. El-Hachemi, J. M. Ribó, *J. Phys. Chem. B* **2004**, 108, 4631. b) B. Z. Packard, D. D. Toptygin, A. Komoriya, L. Brand, *Proc. Natl. Acad. Sci. U.S.A.* **1996**, 93, 11640. c) C. A. Hunter, J. K. M. Sanders, A. J. Stone, *Chem. Phys.* **1989**, 133, 395. d) J. M. Ribó, J. M. Bofill, J. Crusats, R. Rubires, *Chem. Eur. J.* **2001**, 7, 2733.

22 M. Kasha, H. R. Rawls, M. A. El-Bayoumi, *Pure Appl. Chem.* **1965**, 11, 371.

23 D. M. Togashi, S. M. B. Costa, A. J. F. N. Sobral, A. M. d'A. R. Gonsalves, *J. Phys. Chem. B* **2004**, 108, 11344.

24 C. A. Hunter, J. K. M. Sanders, *J. Am. Chem. Soc.* **1990**, 112, 5525.

25 L. L. Shipman, T. M. Cotton, J. R. Norris, J. J. Katz, *Proc. Natl. Acad. Sci. U.S.A.* **1976**, 73, 1791.

26 X. Hu, A. Damjanović, T. Ritz, K. Schulten, *Proc. Natl. Acad. Sci. U.S.A.* **1998**, 95, 5935.